Clim. Past Discuss., 7, 2089–2118, 2011
www.clim-past-discuss.net/7/2089/2011/
doi:10.5194/cpd-7-2089-2011

Climate of the Past Discussions

Productivity response of calcareous nannoplankton in the South Atlantic to the Eocene Thermal Maximum 2 (ETM2)

M. Dedert[1], H. M. Stoll[2,3], D. Kroon[4], N. Shimizu[5], and P. Ziveri[1,6]

[1]Section of Marine Biogeology, Department of Earth Sciences, Faculty of Earth and Life Sciences, Vrije Universiteit Amsterdam, Amsterdam, The Netherlands
[2]Dept. de Geologia, Universidad de Oviedo, Asturias, Spain
[3]Geoscience Department, University of Massachusetts at Amherst, Amherst, MA, USA
[4]School of Geosciences, University of Edinburgh, Edinburgh, UK
[5]Geology and Geophysics Department, Woods Hole Oceanographic Institute, Woods Hole, MA, USA
[6]ICTA, Autonomous University of Barcelona (UAB), Bellaterra, Spain

Received: 27 April 2011 – Accepted: 16 May 2011 – Published: 23 June 2011

Correspondence to: M. Dedert (dedm@falw.vu.nl)

Published by Copernicus Publications on behalf of the European Geosciences Union.

Abstract

The Early Eocene Thermal Maximum 2 (ETM2) at ∼53.7 Ma is one of multiple hyperthermal events that followed the Paleocene-Eocene Thermal Maximum (PETM, ∼55 Ma). In order to reconstruct the primary productivity response to the ETM2 in the South Atlantic, we have analyzed Sr/Ca ratios in various size fractions of bulk sediments and in picked monogeneric populations of calcareous nannofossils. The latter technique of measuring selected nannofossil populations using the ion probe circumvents possible contamination with secondary calcite. Avoiding such contamination is important for interpretation of the nannoplankton productivity record, since diagenetic processes can bias the productivity signal, as we demonstrate for Sr/Ca measurements in the fine (<20 um) and other size fractions obtained from bulk sediments. The paleoproductivity signal as reconstructed from the Sr/Ca ratios appears to be dominantly governed by cyclic orbital forcing. The ∼13 to 21 % increase in Sr/Ca above the cyclic background conditions as measured by ion probe in dominating genera is likely the result of a slightly elevated productivity during ETM2. This high productivity phase is the result of enhanced nutrient supply either from land or from upwelling. Our results show that calcareous nannoplankton productivity was not reduced by environmental conditions accompanying ETM2, but even showed a small increase during the extreme climatic conditions of ETM2.

1 Introduction

The present rapid increase of greenhouse gases in the atmosphere has led to an increased interest in similar events that occurred in the geological past. Studying these events contributes to understanding how increased atmospheric CO_2 concentrations (pCO_2) had and possibly will have an impact on the climate system. Pronounced increases in pCO_2 in the past took place during hyperthermal events, of which the most distinct was the Paleocene-Eocene Thermal Maximum (PETM; ∼55 Ma) (Zachos et al., 1993). Several hyperthermals followed the PETM in the early Eocene (Lourens

CPD
7, 2089–2118, 2011

Productivity response of calcareous nannoplankton

M. Dedert et al.

et al., 2005; Nicolo et al., 2007), showing similar geochemical and biotic characteristics as those during the PETM, such as sea surface temperature increase and a decrease in benthic foraminifera species richness, although smaller in magnitude. One of these hyperthermals is the Eocene Hyperthermal Maximum 2 at ∼53.7 Ma (ETM2) (Lourens et al., 2005) that is characterized by a negative Carbon Isotope Excursion (CIE) of ∼1,5 ‰ and a low carbonate content interval (*Elmo* horizon) resulting from shoaling of the Calcite Compensation Depth (CCD).

Insights into marine primary production obtained from the geological record can add to our understanding of the recovery of the climate system, as increased productivity of marine phytoplankton could have functioned as a negative feedback to high CO_2 concentrations. Calcareous nannoplankton was the key primary producer in marine ecosystems until about 35 Ma (Falkowski et al., 2004). As such, any changes in productivity could have had a significant impact on the climate system through the formation of organic matter and calcite scales. Furthermore, studying the calcareous nannoplankton response to ETM2 gives the opportunity to evaluate whether environmental conditions during the PETM triggered unique responses or that, despite differences in e.g. magnitude (Lourens et al., 2005) and mechanisms (Sexton et al., 2011), calcareous nannoplankton demonstrated analogous changes in productivity.

In this study we use Sr/Ca ratios in nannofossil calcite to reconstruct changes in primary productivity of calcareous nannoplankton in the South Atlantic during ETM2. This geochemical proxy has been shown in culture and field studies to be a good measure for the productivity of coccolithophores (Rickaby et al., 2002; Stoll et al., 2002a, b, 2007a). It is also shown that nutrient availability is the main controlling factor. In addition, Sr/Ca is an ideal proxy to reconstruct productivity changes during ETM2, because of the fact that long residence time of both, Sr and Ca in seawater exceeds the duration of transient climatic events such as hyperthermals. Studies applying this new method have demonstrated increased primary production during upwelling events or in coastal (proximity) settings in both extant and fossil calcareous nannoplankton (Stoll et al., 2007a, b; Auliaherliaty et al., 2009).

CPD
7, 2089–2118, 2011

It is still under debate whether high CO_2 conditions during hyperthermal events have had detrimental effects on calcifying organisms, such as calcareous nannoplankton. Processes involving dissolution and early diagenesis can complicate an accurate interpretation of their fossil record, and could well explain why paleoecological and geochemical productivity reconstructions often give contradictory results (e.g. Stoll and Bains, 2003; Bralower et al., 2004). We therefore use the Sr/Ca records in combination with paleoecological data of well-preserved intervals, i.e. high carbonate sediments, covering the ETM2 event to evaluate the potential influence of extreme climatic conditions on calcareous nannoplankton productivity.

2 Methods and materials

Samples were taken from Hole 1265A, one of the shallowest sites (∼1500 m paleodepth) taken on a depth transect recovered on the Walvis Ridge during Ocean Drilling Program Leg 208 (Zachos et al., 2004). The CIE, an interval characterized by a gradual shift towards lighter $\delta^{13}C$ values, signifies the release of ∼440–1600 Gt of carbon in case of methane ($\delta^{13}C$ −60 ‰) or ∼1000–4500 Gt carbon in case of organic carbon ($\delta^{13}C$ −22 ‰) into the biosphere (Ridgwell, 2007). The propagation of this carbon into the marine system resulted in shoaling of the CCD and a drop in $CaCO_3$ content from generally high (∼90 to 95 %) to ∼54 %. This effect on the sediment archive was identified by shipboard MS and reflection data as a distinct layer, called the *Elmo* horizon (Lourens et al., 2005) (Fig. 2b).

We measured the Sr/Ca ratio by ion probe in four individual taxa, each with distinct environmental preferences. We applied the method developed by Stoll et al. (2007c) that makes it possible to measure Sr/Ca ratios in monogeneric samples of nannofossil calcite, allowing for reconstruction of productivity response of individual nannofossil taxa without geochemical contamination by carbonate of other origin, or influence of alteration of primary calcite. In addition, we measured the Sr/Ca ratios in various nannofossil size fractions separated from bulk sediments that allows for the qualitative reconstruction of productivity trends at a higher resolution and over a longer time interval. The combination of Sr/Ca results obtained by ion probe for individual taxa and in nannofossil size fractions by ICP-AES is fundamental for quantifying the amounts of secondary calcite present in the nannofossil size fractions. This suite of analyses allows us to determine to what extent diagenetic processes have biased the Sr/Ca productivity trends in sediments covering the ETM2 interval and to obtain a better perspective on how the ETM2 productivity signal relates to background productivity trends.

The method for isolating nannofossils for Sr/Ca analyses is described in detail by Stoll et al. (2007b) and Stoll and Shimizu (2009). We have picked both placoliths, the circular plates (coccoliths) common to modern dominant genera of coccolithophores, such as extant species *Emiliania huxleyi* or *Gephyrocapsa oceanica*, as well as several genera of nannoliths, which are non-coccolith morphologies produced by haptophytes, or objects produced by biologically distinct, but ecologically similar phytoplankton groups (Bown et al., 2004). Common placolith-bearing genera from our site include *Coccolithus pelagicus*, *Toweius*, and *Chiasmolithus*. Common nannoliths include *Discoaster* and *Sphenolithus*. In addition, we picked populations of the holococcolith *Zygrhablithus*. For each genus a population of 15 to 20 specimens was picked together with individual specimens of *Discoaster*. Samples were measured using a Cameca IMS3f secondary ion mass spectrometer (SIMS) at the Northeast National Ion Microprobe Facility at Woods Hole Oceanographic Institute.

Size fractions were obtained through a combination of separation methods as described by Minoletti et al. (2001) and Stoll and Ziveri (2002). The application of the filtration technique as described by Minoletti et al. (2001) to bulk sediments resulted in the following size fractions: bulk fine (<20 µm), 10–20 µm and 5–8 µm. Further separation of the 10–20 µm size fraction using the settling/ decanting technique described in Stoll and Ziveri (2002) resulted in a discoaster fraction, to which *Discoaster* is the dominant contributor to the carbonate.

Size fraction Sr/Ca ratios were measured using the simultaneous dual ICP-AES (Thermo ICAP DUO 6300) at the University of Oviedo. Sr/Ca measurements were

CPD
7, 2089–2118, 2011

made using radial detection of Sr 421.5 nm and Ca 315 nm. Calibration was conducted using three standards with constant Ca concentrations and different Sr/Ca ratios, which vary from 0.75 to 4 mmol mol^{-1}, following the intensity ratio method described by Villiers et al. (2002). For the calculation of the contribution of abiogenic calcite to the size fractions, we used the Sr/Ca value of 0.13 that was measured in abiogenic needles found at Site 1209 (Stoll et al., 2007c) as an end-member for abiogenic calcite. The relative contribution to each size fraction by the taxa analyzed by ion probe, and the ion probe Sr/Ca data for these taxa were used to calculate the average biogenic end-member. These end-members together with the Sr/Ca size fraction data measured by ICP-AES allowed for the calculation of the amount of secondary calcite (overgrowth) present in the discoaster and the 5–8 µm fractions.

Nannofossil assemblages and size fractions were analyzed by light microscope (LM) at 1600 magnification and Scanning Electron Microscope (SEM) at the Free University Amsterdam and the Natural History Museum London. For relative abundance counts, samples were taken every cm from 14 cm below (277,59 mcd) the ETM2 horizon to 11 cm above (277,27 mcd) the horizon and every five cm outside this interval. Smear slides were prepared using standard techniques. The nannofossils were identified to genus level; about 300–400 specimens were counted per interval. Carbonate mass contribution of carbonate by liths of each genus to the total mass of a specific size fraction was calculated following Young and Ziveri (2000), with nannofossil weights per nannolith taken from Stoll and Bains (2003).

3 Results

3.1 Nannofossil preservation

SEM analyses revealed severe overgrowths covering the nannoliths *Discoaster* and *Tribrachiatus*, and the holococcolith *Zygrhablithus.* The placoliths of *Coccolithus*, *Chiasmolithus* and *Toweius* are not significantly overgrown (Plate 1 Preservation nannofossils). The amount of overgrowth on liths of *Discoaster, Tribrachiatus* and *Zygrhablithus* is strongly correlated to the carbonate content of the sediments, with the degree of overgrowth decreasing within low carbonate content sediments of the *Elmo* horizon. The preservation of particularly the liths of placolith taxa decreases within the CIE, i.e. increasingly affected by dissolution, and is poor within low carbonate content sediments of the *Elmo* horizon.

3.2 Sr/Ca ratios in picked populations

The Sr/Ca ratios in picked populations of both *Coccolithus* and *Toweius* decrease to a minimum at 277.65 mcd, followed by an increase in *Coccolithus* a few centimeters below the onset of the CIE (Fig. 2; as measured in the fine bulk fraction (<20 µm)). The Sr/Ca ratios in *Toweius* increase at the onset of the carbon isotope excursion (Fig. 2a). During the CIE, the Sr/Ca in *Coccolithus* and *Toweius* further increases by ∼13 and 21 %, respectively, compared to maximum values before and after the event. *Chiasmolithus* doesn't show a significant response in the ETM2 interval, except for a small increase prior to the CIE that coincides with the increase in *Coccolithus* and *Toweius*. High Sr/Ca ratios in *Coccolithus*, *Toweius* and *Chiasmolithus* coincide with light δ^{13}C-values measured below and in the *Elmo* horizon (Fig. 2a). After the CIE, the Sr/Ca ratios in *Coccolithus* remain stable until the C- isotope signal has returned to pre- ETM2 values. The Sr/Ca in *Toweius* drops to a second minimum comparable to the low Sr/Ca in *Toweius* preceding the event, followed by a return to the initial pre-excursion values during the recovery period (Fig. 2a). The Sr/Ca values measured by ion probe show no correlation with changes in carbonate content across the ETM2 interval (Fig. 2b).

Accurate measurements of the Sr/Ca ratios in picked populations of *Discoaster* or *Zygrhablithus* were not possible, due to the amount of overgrowth present on the nanoliths. In *Discoaster* specimens that were picked individually the Sr/Ca ratios could be measured by gradually ablating through the layers of overgrowth. The Sr/Ca measured in individual specimens of *Discoaster* is higher in the two specimens present in

CPD
7, 2089–2118, 2011

the *Elmo* horizon, compared to the Sr/Ca measured in individual specimen below and above the ETM2 (Fig. 2). No individual specimens of *Zygrhablithus* were picked.

3.3 Sr/Ca in different size fractions

The applied separation techniques resulted in various size fractions with distinctly different species composition. The bulk fine fraction (<20 µm) represents the original assemblage composition, whereas the application of separation techniques resulted in a discoaster fraction to which discoasters contribute ∼60 % of the carbonate mass. The carbonate mass contribution to the 5–8 µm size fraction is dominated by small morphotypes (∼60–80 %) of mostly placoliths together with a significant contribution (10–25 %) by *Zygrhablithus* (Fig. 3b), except for samples within the *Elmo* horizon, when small nannoliths of *Discoaster* become a major contributor.

The various Sr/Ca profiles based on different size fractions follow the Sr/Ca trends as measured in *Coccolithus* and *Toweius* via ion probe (Fig. 3a), although values are generally lower. The Sr/Ca in the discoaster fraction decreases at the onset of the CIE (Fig. 3b). On average, the contribution of abiogenic calcite to the 5–8 µm fractions is ∼30 %, whereas the contribution to the discoaster fraction is ∼50 %. The contribution of abiogenic calcite to the 5–8 µm size fraction decreases sharply in the *Elmo* horizon, whereas contribution of overgrowth to the discoaster fraction remains ∼50 %. Furthermore, abiogenic calcite appears to increase just below and above the *Elmo* horizon in the 5–8 µm size fraction (Fig. 3c).

3.4 Long-term Sr/Ca trends in bulk fine sediments

Long-term trends in Sr/Ca measured in bulk fine (<20 µm) sediments reveal a cyclic forcing, possibly precessional, as was identified in δ^{13}C records (Stap et al., 2009), although Sr/Ca trends are less salient in proximity of the ETM2 interval (precession cycle numbers one, two and five; Fig. 4a). Bulk fine Sr/Ca shows no direct correlation with the carbonate dissolution as calculated by Stap et al. (2009) (Fig. 4a). The

CPD
7, 2089–2118, 2011

Sr/Ca values measured in bulk fine sediments from within the *Elmo* horizon are higher than the Sr/Ca values measured during other cyclic peaks in productivity. The clearest cyclic-driven increase in Sr/Ca is recorded following the ETM2 during cycles number seven and eight, with a difference between minima and maxima in Sr/Ca of ~23 %. An interval of relatively high Sr/Ca is present between cycle five and six (Fig. 4a). A change in assemblage composition, e.g. due to dissolution, may in part explain variations in Sr/Ca measured in the bulk fine fraction. However, the species composition of the nannofossil assemblage across the H2 event (Stap et al., 2009) does not change significantly (Fig. 4b).

3.5 Changes in nannofossil abundances

The relative abundances of the different nannofossil taxa show pronounced changes within the dissolution interval (Fig. 5), e.g. a sharp increase of the dissolution-resistant *Discoaster* and a drop in *Toweius* abundance that is strongly correlated to the CIE (Fig. 5; Dedert et al., 2011). The relative abundances of the most abundant nannofossil in the assemblages, *Coccolithus*, show a sharp increase within the CIE ~10 ka prior to the *Elmo* horizon (Fig. 5).

4 Discussion

4.1 Geochemical records of environmental changes

We used Sr/Ca ratios in nannofossil calcite to identify productivity trends across the ETM2 interval. However, because secondary calcite formed during diagenetic processes possibly influences productivity signals, we first evaluate how these processes may have obscured primary Sr/Ca variations. Our evaluations indicate that the least altered materials are placoliths which were picked for ion probe analysis and thus these provide the most reliable data on productivity changes. Some specific size fractions, in

CPD
7, 2089–2118, 2011

contrast, have geochemical variations which have been significantly affected by variable diagenesis.

4.1.1 Primary versus diagenetic geochemical signals

Diagenetic processes can alter the geochemical composition of carbonate sediments and potentially distort climatic signals preserved in nannofossil carbonate (Dedert et al., 2011). However, several lines of evidence suggest that temporal Sr/Ca variations observed in individually picked placolith nannofossils analyzed by ion probe are not artifacts of differential diagenesis. Firstly, SEM analyses showed that the placoliths (e.g. *Coccolithus*, *Toweius*, and *Chiasmolithus*) are not covered by appreciable overgrowth, which has made obtaining the Sr/Ca in the primary calcite (core signal) by the ion probe possible. Secondly, the applied method of picking individual nannofossils enables to selectively isolate specimens that are well-preserved. In addition, the difference in Sr/Ca response in the four species shows that dissolution, which is common to all sediment components, has not been the dominant control on temporal variations in the coccolith Sr/Ca ratios. For example, variations in Sr/Ca in *Coccolithus* preceding the onset of dissolution (Fig. 2) differ from the Sr/Ca in *Toweius*, indicating that these Sr/Ca values are not the result of diagenetic processes, as for example could be expected in the *Elmo* Horizon as a result of reduced presence of overgrowth. Furthermore, there is no correlation between the $CaCO_3$ and Sr/Ca measured in the different taxa (Fig. 2b).

In contrast to the monogeneric Sr/Ca data obtained by ion probe, geochemical signals in the different size fractions might have been affected by differential diagenesis, as variable abundances of *Discoaster* and *Zygrhablithus* and the strong secondary overgrowth on these genera resulted in varying amounts of abiogenic calcite to the size fractions. A clear example of the presence of this overgrowth and its impact on geochemical signals is shown in the Sr/Ca ratios that were measured in the different size fractions. Abiogenic calcite has lower Sr/Ca ratios than biogenic calcite, which results from the loss of Sr to porewaters during diagenetic recrystallisation (Richter and Liang, 1993; Stoll and Schrag, 2001). As a result, the lower Sr/Ca in particularly the

CPD
7, 2089–2118, 2011

discoaster fraction, when compared to the Sr/Ca obtained by ion probe, indicates an important contribution of abiogenic calcite to this size fraction.

One estimate of the amount of secondary calcite can be attained by comparing the total amount of carbonate from these taxa that makes up their shell with the proportion of secondary calcite. The most heavily overgrown specimens of *Discoaster*, *Tribrachiatus* and *Zygrhablithus* appear to be composed of as much as 50 % to 70 % of secondary calcite, according to SEM analysis and geochemical heterogeneity in profiles of overgrown nannoliths completed with the ion probe (Dedert et al., 2011). The abundances of these heavily overgrown taxa account for ~ 20 to 40 % of the carbonate mass in the 5–8 µm fraction, whereas contribution to the discoaster fraction is ~70 to 80 %. Consequently, the overgrowth on these taxa could result in ~10 to 30 % of the calcite to the 5–8 µm fraction coming from abiogenic overgrowth, and ~35 to 40 % of the calcite present in the discoaster fraction coming from abiogenic overgrowth. In addition to overgrowth, other sources of abiogenic calcite that further contributed to the size fractions could include small amounts of overgrowth present on placoliths and abiogenic calcite blocks.

The difference in Sr/Ca ratios between the well-preserved placoliths analyzed by ion probe and the sediment size fractions provides a second indication of the degree of overgrowth and its variability. As inferred from the mass balance calculations above, the discoaster fraction contains a much higher percentage of overgrowth than the 5–8 µm fraction. However, the degree of overgrowth estimated from the contrast between the ion probe and size fraction chemistry is much larger compared to that from the mass balance of the highly overgrowth taxa. While the temporal trends are probably robust, a systematic overestimation in the degree of secondary calcite could arise if the Sr/Ca ratio of the diagenetic end-member has been overestimated. Because seawater Sr/Ca ratios are not well-constrained during the early Cenozoic, there is no independent estimate of the expected ratio of equilibrium abiogenically precipitated calcite. Also, the nannofossil size fractions include other genera of which the Sr/Ca values are unknown from ion probe. If these lesser contributors had lower Sr/Ca ratios than the dominant

CPD
7, 2089–2118, 2011

genera, the degree of overgrowth could be overestimated. Consequently, while the temporal trends and the different degrees of overgrowth in the size fractions can be inferred with confidence, the estimates of overgrowth have significant uncertainty.

The high contribution of abiogenic calcite to the discoaster fraction compared with the 5–8 µm size fraction also became evident by the δ^{18}O measurements in the discoaster fraction, which were biased towards heavier δ^{18}O values (Dedert et al., 2011). Furthermore, the δ^{18}O data suggest an increase in abiogenic calcite to this fraction prior to the *Elmo* horizon, which is also indicated by the downward trend in discoaster fraction Sr/Ca during the onset of the CIE. Such an increase probably occurred during changes in post-depositional conditions accompanying the onset of the ETM2 event, i.e. shoaling of the CCD (Lourens et al., 2005). The enhanced diagenetic alterations of biogenic carbonate thus may have biased the geochemical signals at the onset of the ETM2 at this site. Similarly, the higher contribution of abiogenic calcite to the 5–8 µm size fractions just above and below the *Elmo* horizon (Fig. 3c) could have dampened the Sr/Ca productivity trend measured in these fractions. The limited number of Sr/Ca measurements on individual *Discoaster* specimens does not allow us to draw any conclusions on overgrowth variations for the discoaster fraction across the ETM2 interval.

4.1.2 Productivity and ecological changes

Because the ion probe geochemical data appear minimally affected by diagenesis, we infer the overall pattern of productivity and ecological change from the Sr/Ca variations in the dominant genera of the sediments, *Coccolithus* and *Toweius*, since these two genera exhibit similar overall temporal trends in our record, consistent with the similarities in their ecological preferences. First of all, there is a clear background variation in productivity of both *Coccolithus* and *Toweius* prior to the first C-isotopic shift that marks the ETM2 (with a maximum at 277.75 mcd and minimum at 277.65 mcd) (Fig. 2c). The decrease in Sr/Ca prior to the ETM2 measured in both species suggests that nutrient availability temporarily decreased, and the transient increase of Sr/Ca in both taxa just

CPD
7, 2089–2118, 2011

prior to the carbon isotopic excursion is thus likely to be a return to the initial productivity rates rather than a "precursor" related to environmental conditions during ETM2. During the initial recovery, the minima in Sr/Ca in *Toweius* may also reflect the same cyclic forcing of productivity observed prior to the ETM2 event.

The productivity responses of minor species are less salient. In *Chiasmolithus* a single sample indicates potentially higher productivity in this genus during the ETM2 onset (Fig. 2c). The SEM analyses showed that nannofossil specimens of *Chiasmolithus* are not significantly overgrown, implying that the productivity signal obtained from the Sr/Ca analyses is a genuine productivity response of *Chiasmolithus*, and is not biased by secondary calcite as was the case for picked populations of *Zygrhablithus* and *Discoaster*. Similar transient increases in *Chiasmolithus* productivity at the onset of hyperthermal events have been observed for the PETM in the Southern Ocean ODP Site 690 (Stoll et al., 2007c), and in the South Atlantic at Walvis Ridge ODP Site 1263 (Dedert et al., 2011). The brief, transient response may reflect that *Chiasmolithus* is a species that is better adapted to mesotrophic cold- water environments (Bralower, 2002), and the environmental conditions attained at the peak ETM2 conditions at Site 1265 may not have been favorable for an optimal growth of this taxon. Mutterlose et al. (2007) found that *Chiasmolithus* did not change much in abundance at Site 1260 during the PETM, suggesting limited environmental sensitivity of the genera at this site.

Interpretation of Sr/Ca ratios in discoasters is, in addition to the high degree of secondary overgrowth on this taxon, further complicated by the small number of individuals represented by the analyses, since individual liths rather than populations were analyzed. Two individual discoasters during the ETM2 event, present in the *Elmo* horizon (Fig. 2b,c), feature higher core Sr/Ca ratios (Dedert et al., 2011), which could be interpreted as nutrient-stimulation of productivity in this genera, as observed for *Coccolithus* and *Toweius*. However, the SEM images and geochemical data presented in that study suggest that discoasters are strongly overgrown with secondary calcite. If secondary overgrowth on discoasters were reduced during the ETM2 event, then the greater prevalence of primary high Sr/Ca calcite may have elevated the Sr/Ca ratios.

CPD
7, 2089–2118, 2011

Thus it is not possible to confidently interpret productivity variations of *Discoaster* at this location.

The high productivity peaks measured in the different size fractions as well as the ion probe data correlate with precessional/ orbital cycling as identified by Stap et al. (2009) (Fig. 4a). However, attempts to identify the longer term context of productivity changes, by using extended Sr/Ca records in bulk fine sediments, are complicated because diagenetic factors do potentially affect the Sr/Ca signals in the bulk fraction. Overall, long-term Sr/Ca productivity trends measured in the bulk fine sediments do not show a clear correlation with the precession cycles in the proximity of the ETM2. Stratigraphically above the ETM2 in our bulk Sr/Ca record, the precession-driven variations in productivity are more clearly expressed during precession cycles number six and seven (Fig. 4a). This could imply that productivity variations in response to precessional forcing during time intervals other than the ETM2 may not have been as pronounced.

More likely, the bulk Sr/Ca may have less faithfully recorded the productivity trends compared to the 5–8 µm size fraction due to the varying contribution of secondary calcite to the bulk fine fraction. For example, productivity trends particularly in the proximity of the ETM2 interval appear to be biased. During the ETM2 interval, climatic conditions may have caused diagenetic processes to be more variable through e.g. alternating warm oversaturated deep waters with enhanced diagenetic overgrowth and suppressed Sr/Ca ratios in sediments, with more acidified undersaturated deep waters with less overgrowth and closer fidelity to the higher primary Sr/Ca ratios. The peak in Sr/Ca measured during the ETM2 that strongly correlates with the dissolution interval may be an example of the latter process. Better preservation and consequently less diagenetic alteration of nannofossil calcite may also explain the high Sr/Ca values in the interval between precession cycle four and five, when the dissolution of $CaCO_3$ was relatively low (Fig. 4a). If, as our ETM2 Sr/Ca data suggests, precessional cycles were accompanied by increased productivity, this may have led to an increased burial of organic matter to the deeper waters. If the degradation of this organic matter occurred deep enough in the sediment column to release CO_2 in closed conditions and

CPD
7, 2089–2118, 2011

promoted greater overgrowth of carbonate (Barker et al., 2006), it may have attenuated the primary Sr/Ca productivity signal.

Another possibility is that the Sr/Ca trends are caused by changes in the assemblage composition. However, contrary to the changes in assemblage composition during the ETM2, selected counts across H2, an event succeeding ETM2 with similar characteristics (Stap et al., 2009) show that the species composition does not change significantly (Fig. 4b). As such, the Sr/Ca ratios in the bulk fine fraction are unaffected by potential influence of nannofossil species-specific partitioning of Sr.

4.2 Climatic reconstructions using nannofossil assemblages: dissolution versus paleoecology

The Sr/Ca productivity trends presented in this study appear to contradict those inferred from changes in nannofossil assemblages for this site, in that meso-trophic and eutrophic placoliths decrease in abundance. However, the response of calcareous nannoplankton to hyperthermal events in the geological past is especially difficult to reconstruct using census counts, since these events are often accompanied by a pronounced dissolution of the calcareous components. During ETM2 at Site 1265, the drop in $CaCO_3$ % from ∼90 % to ∼53 % signifies a loss of about 70 % of the original carbonate content (Broecker, 2003) to a loss of ∼90 % as calculated by Stap et al. (2009). The high concentration of fragments of placoliths present in the nannofossil assemblages indicate that dissolution has had a major impact on the abundances of particularly these more solution-prone placolith genera (Perch-Nielsen, 1985).

At most sites, nannofossil assemblages across the PETM demonstrate a shift towards a composition indicative of more oligotrophic conditions (Monechi et al., 2000; Bralower, 2002; Tremolada and Bralower, 2004; Kahn and Aubry, 2004; Mutterlose et al., 2007). Similarly for the ETM2 at Site 1265, concomitant with the CIE and more importantly the *Elmo* horizon, variations in relative abundances of several nannofossil taxa show a marked change, most notably a sharp increase in *Discoaster* and decreases in *Toweius* (Fig. 5; Dedert et al., 2011). While these changes were originally inferred to result from the warmer and more oligotrophic conditions during the PETM, there is increasing recognition of a strong and potentially dominant control of selective dissolution (Raffi and deBernardi, 2008; Jiang and Wise, 2009). In fact, multi-proxy analyses of assemblage records at various sites suggest that productivity was not negatively affected by environmental conditions associated with the PETM (Gibbs et al., 2010).

Although selective dissolution may influence the relative abundances of the various placolith species during ETM2, in some cases there is clear evidence for primary ecological shifts. An increase in *Coccolithus* prior to the dissolution when carbonate content was still ∼90 %, is likely to reflect a real shift in photic zone ecology. *Coccolithus* is generally regarded to be a warm-water species (Aubry, 1998) with high abundance in eutrophic settings (Jiang and Wise, 2006). Thus this increase would suggest more eutrophic conditions to prevail prior to ETM2. A comparable increase in eutrophic species just prior to the PETM was observed during several studies (Bralower, 2002; Tremolada and Bralower, 2004; Jiang and Wise, 2006). In one such study in the Weddell Sea, an increased abundance of the eutrophic taxon *Biscutum* just before the PETM correlates to a warming signal found in the O-isotopes (Bralower, 2002), which is ascribed to a possible pulse of increased upwelling. A similar correlation is found between increasing relative abundances of *Coccolithus* and the transient warming found in the O-isotopes prior to the *Elmo* horizon when $CaCO_3$ was still ∼90 % (Fig. 5). These correlations may result from an increased productivity of this eutrophic species just prior to the event, and as for the Sr/Ca productivity signals, implies that the ETM2 was accompanied by an overall sustained and slightly increased productivity.

4.3 Mechanisms for stimulating productivity

The amplitude of Sr/Ca measured in the dominant genera *Coccolithus* and *Toweius* both prior and during the ETM2 suggests that productivity in response to ETM2 did not change significantly. The decrease just prior to ETM2 in both species and in *Toweius* just after ETM2 however, implies that a cyclic forcing is controlling the productivity at this site.

Nutrient concentrations at the Walvis Ridge during ETM2 are likely to have mainly been affected by changes in upwelling intensity and/ or weathering rates, making changes in environmental conditions as a result of precessional forcing a strong candidate for the cyclic productivity changes observed in this Early Eocene record. Precessional forcing is a dominant factor in controlling the intensity and zonality of the trade winds, which in turn affects upwelling intensity. Wind intensity determines the degree of transport of cold upwelled water in filaments over the Walvis Ridge (West et al., 2004), with stronger upwelling occurring during precession maxima resulting from stronger SE trade winds. Trade wind modulated productivity in this region of the South Atlantic has been observed for the Quaternary (Schneider et al., 1996; Jahn et al., 2003). Furthermore, extant coccolithophore assemblages in the Southwestern African margin, similar to other upwelling regions, are largely governed by changes in upwelling intensity (Boeckel and Baumann, 2004; Ziveri et al., 1995; Ziveri and Thunell, 2000). However, modeling studies are not conclusive about whether wind strength would have intensified during hyperthermal events (Huber and Sloan, 1999, 2000, 2001; Sloan and Huber, 2000). In addition to upwelling intensity, increased weathering is a mechanism that has been recognized as a potentially important negative feedback to the high pCO_2 during the PETM (Bowen et al., 2004). Consequently, an increased primary productivity may have enhanced CO_2 drawdown, and elevated carbonate removal in carbonate burial (Zachos et al., 2005).

It is difficult to clearly identify which mechanism dominantly controlled the productivity at this site, and it is possible that a combination of changes in the intensity of both mechanisms, upwelling and weathering, resulted in the productivity signal reconstructed for Site 1265 during ETM2. However, the response of productivity to ETM2 in *Toweius*, and to a lesser extent in *Coccolithus*, appears to exceed the range of variation immediately before or after the ETM2. This suggests that the environmental changes of the ETM2 triggered a unique maximum in nutrient-stimulated productivity at this site, at least in the context of the cycle immediately preceding and following the ETM2 event, which is consistent with the weathering hypothesis that hyperthermal events are accompanied by increased input of nutrients into the marine ecosystem. However, in case of intensified wind systems, an increase in upwelling rates might have had a similar effect on calcareous nannoplankton productivity, and can not be ruled out.

4.4 Implications for climatic feedbacks

The results presented here and previous studies (Stoll et al., 2007c; Stoll and Bains, 2003) show that productivity during the hyperthermal events remained rather constant or even increased in different oceanic settings. The question that remains is how or if the higher pCO_2 would have affected the calcification and growth of calcareous nannoplankton.

During the ETM2 period of inferred higher CO_2, there is no evidence of a productivity crisis of calcifying algae, consistent with a number of studies on the PETM (Gibbs et al., 2006; Stoll et al., 2007c). In addition, the rate of CO_2 addition during the ETM2 is still not clear, although was recently estimated to have taken place over ~20 ka (Stap et al., 2010), thus the degree of surface acidification may have been minor if carbon was added gradually. The impact that dissolution has had on the assemblage composition during ETM2 explains why the paleoecological signal found in nannofossil assemblages often contrasts with the productivity signal reconstructed from Sr/Ca ratios (Stoll and Bains, 2003; Bralower et al., 2004). The increased nutrient availability as reconstructed from nannofossil assemblages prior to, e.g. the PETM, as found during this study and by Bralower (2002), Tremolada and Bralower (2004) and Jiang and Wise (2006) may actually signify the true climate signal that is not affected by nannofossil dissolution.

The net CO_2 effect of increased productivity of coccolithophore groups is still ambiguous. Coccolith calcification decreases surface ocean alkalinity, which reduces CO_2 uptake by the ocean. Since coccolithophore productivity likely represents the overall marine primary productivity during the Paleogene, any change would have affected the

CO_2 drawdown by the oceans. Yet, the coccolith mineral can play an important role in ballasting organic carbon export to the deep ocean (Klaas and Archer, 2002; Ziveri et al., 2007), and thereby strengthening the biological pump uptake of CO_2 from the atmosphere. In the Paleogene, when coccoliths were the main ballast minerals, the latter might have been of greater importance, and contributed to deep ocean DOC storage in the Early Eocene (Sexton et al., 2011).

5 Summary

The calcareous nannoplankton productivity as reconstructed from Sr/Ca productivity signals obtained by ion probe indicate a sustained and slight increase in productivity during the ETM2. Long-term productivity reconstructions using the bulk fine fraction can be biased by diagenetic processes that attenuate the productivity signals. Nonetheless, variations in Sr/Ca across the ETM2 interval and at certain intervals in the bulk fine Sr/Ca record imply a cyclic forcing on the productivity. The additional increase in productivity during ETM2 might be the result of increased weathering rates, more intensified upwelling, or a combination of both mechanisms.

Acknowledgements. This work was supported by the Darwin Center for Biogeosciences (MD and PZ), the National Science Foundation (NSF EAR-0628336 to HMS) and the Spanish Minister of Science and Innovation (MCINN AD122622). We thank Saskia Kars and Jeremy Young for SEM analyses, Claudia Agnini for taxonomic assistance, Lucy Stap and Luc Lourens for insightful discussions and close collaboration, and Gerald Ganssen and Luc Lourens for comments to an earlier version that helped to improve this manuscript.

Author contributions: this manuscript represents part of the PhD thesis of MD at the Free University Amsterdam (VUA) under active direction of H. M. S., P. Z. and D. K. Size fraction separation and assemblage counts were completed by M. D. at VUA. Coccolith picking and elemental geochemistry of size fractions was completed by M. D. at Oviedo University under direction of H. S. Ion probe analyses were conducted by H. S. and N. S.

References

Aubry, M. P.: Early Paleogene calcareous nannoplankton evolution: a tale of climatic amelioration, in: Late Paleocene Early Eocene climatic and biotic events in the marine and terrestrial records, edited by: Aubry, M. P., Lucas, S. G., and Berggren, W. A., 158–203, Columbia University Press, New York, 1998.

Auliaherliaty, L., Stoll, H. M., Ziveri, P., Malinverno, E., Triantaphyllou, M., Stravrakakis, S., and Lykousis, V.: Coccolith Sr/Ca ratios in the eastern Mediterranean: production versus export processes, Mar. Micropaleontol., 73, 196–206, 2009.

Barker, S., Archer, D., Booth, L., Elderfield, H., Henderiks, J., and Rickaby, R. E. M.: Globally increased pelagic carbonate production during the Mid-Brunhes dissolution interval and the CO_2 paradox of MIS II, Quaternary Sci. Rev., 25, 3278–3293, 2006.

Boeckel, B. and Baumann, K. H.: Distribution of coccoliths in the surface sediments of the south-eastern South Atlantic Ocean: ecology, preservation and carbonate distribution, Mar. Micropaleontol., 51, 301–320, 2004.

Bowen, G. J., Beerling, D. J., Koch, P. L., Zachos, J. C., and Quattlebaum, T.: A humid climate state during the Paleocene/Eocene Thermal Maximum, Nature, 432, 495–499, 2004.

Bown, P. R., Lees, J. A., and Young, J. R.: Calcareous nannoplankton evolution and biodiversity through time, in: Coccolithophores: from molecular processes to global impact, edited by: Thierstein, H. R. and Young, J. R., 481–508, Springer, New York, 2004.

Bralower, T. J.: Evidence for surface water oligotrophy during the Paleocene-Eocene Thermal Maximum: Nannofossil assemblage data from Ocean Drilling Program Site 690, Maud Rise, Weddell Sea, Paleoceanography, 17, 1023, doi:10.1029/2001PA000662, 2002.

Bralower, T. J., Kelly, D. C., and Thomas, D. J.: Sr/Ca records of productivity during the PETM of the Weddell Sea: Comment, Paleoceanography, 19, PA1014, doi:10.1029/2003PA000953, 2004.

Broecker, W. S.: The oceanic $CaCO_3$ cycle, in: Treatise on Geochemistry, Vol. 6, The oceans and marine geochemistry, edited by: Elderfield, H., 529–549, Pergamon, Oxford, UK, 2003.

Dedert, M., Stoll, H. M., Kars, S., Young, J. R., Kroon, D., Shimizu, N., and Ziveri, P.: Overgrowth and dissolution affecting nannofossil assemblages covering hyperthermal events: implications for geochemical and palaeoecological analyses and interpretation, in preparation, 2011.

De Villiers, S., Greaves, M., and Elderfield, H.: An intensity ratio calibration method for the

accurate determination of Mg/Ca and Sr/Ca of marine carbonates by ICP-AES, Geochem. Geophys. Geosyst., 3, doi:10.1029/2001GC000169, 2002.
Falkowski, P. G., Katz, M. E., Knoll, A. H., Quigg, A., Raven, J. A., Schofield, O., and Taylor, F. J. R.: The evolution of modern eukaryotic phytoplankton, Science, 305, 354–360, 2004.
Gibbs, S. J., Bralower, T. J., Bown, P. R., Zachos, J. C., and Bybell, L. M.: Shelf and open-ocean calcareous phytoplankton assemblages across the Paleocene-Eocene Thermal Maximum: implications for global productivity gradients, Geology, 34(4), 233–236, 2006.
Gibbs, S. J., Stoll, H. M., Bown, P. R., and Bralower, T. J.: Ocean acidification and surface water carbonate production across the Paleocene–Eocene Thermal Maximum, Earth Planet. Sc. Lett., 295(3–4), 583–592, doi:10.1016/j.epsl.2010.04.044, 2010.
Huber, M. and Cirbus Sloan, L.: Climatic responses to tropical sea surface temperature changes on a "Greenhouse" Earth, Paleoceanography, 15(4), 443–450, 2000.
Huber, M. and Cirbus Sloan, L.: Heat transport, deep waters, and thermal gradients: coupled simulation of an Eocene "greenhouse" climate, Geophys. Res. Let., 28, 3481–3484, 2001.
Huber, M. and Sloan, L. C.: Warm climate transitions: a general circulation modeling study for the Late Paleocene Thermal Maximum (~56 Ma), J. Geophys. Res., 104(D14), 16633–16655, 1999.
Jahn, B., Donner, B., Muller, P. J., Röhl, U., Schneider, R. R., and Wefer, G.: Pleistocene variations in dust input and marine productivity in the northern Benguela Current: evidence of evolution of global glacial-interglacial cycles, Palaeogeogr. Palaeocl., 193(3–4), 515–533, 2003.
Jiang, S. and Wise Jr., S. W.: Surface-water chemistry and fertility variations in the tropical Atlantic across the Paleocene-Eocene Thermal Maximum as evidenced by calcareous nannoplankton from ODP Leg 207, Hole 1259B, Revue de Micropaleontologie, 49, 227–244, 2006.
Jiang, S. and Wise Jr., S. W.: Distinguishing the influence of diagenesis on the paleoecological reconstruction of nannoplankton across the Paleocene-Eocene Thermal Maximum: an example from the Kerguelen Plateau, Southern Indian Ocean, Mar. Micropaleontol., 72(1–2), 49–59, 2009.
Kahn, A. and Aubry, M.-P.: Provincialism associated with the Paleocene-Eocene Thermal Maximum: temporal constraint, Mar. Micropaleontol., 52, 117–131, 2004.
Klaas, C. and Archer, D.: Association of sinking organic matter with various types of mineral ballast in the deep sea: implications for the rain ratio, Global Biogeochem. Cy., 16(4), 1116, doi:10.1029/2001GB001765, 2002.

Lourens, L. J., Sluijs, A., Kroon, D., Zachos, J. C., Thomas, E., Rohl, U., Bowles, J., and Raffi, I.: Astronomically pacing of late Palaeocene to early Eocene global warming events, Nature, 435, 1083–1087, 2005.

Monechi, S., Angori, E., and von Salis, K.: Calcareous nannofossil turnover around the Paleocene-Eocene transition at Alamedilla (southern Spain), B. Soc. Geol. Fr., 171, 477–489, 2000.

Minoletti, F., Gardin, S., Nicot, E., Renard, M., and Spezzaferri, S.: A new experimental protocol for granulometric separation of calcareous nannofossil assemblages: palaeoecological and geochemical applications, B. Soc. Geol. Fr., 172(4), 437–446, 2001.

Mutterlose, J., Linnert, C., and Norris, D.: Calcareous nannofossils from the Paleocene-Eocene Thermal Maximum of the equatorial Atlantic (ODP Site 1260B): evidence for tropical warming, Mar. Micropaleontol., 65, 13–31, 2007.

Nicolo, M. J., Dickens, G. R., Hollis, C. J., and Zachos, J. C.: Multiple early Eocene hyperthermals; their sedimentary expression on the New Zealand continental margin and in the deep sea, Geology, 35(8), 699–702, 2007.

Perch-Nielsen, K.: Cenozoic calcareous nannofossils, in: Plankton Stratigraphy, edited by: Bolli, H. M., Saunders, J. B., and Perch-Nielsen, K., 427–554, Cambridge University Press, Cambridge, 1985.

Raffi, I. and de Bernardi, B.: Response of calcareous nannofossils to the Paleocene-Eocene Thermal Maximum: observations on composition, preservation and calcification in sediments from ODP Site 1263 (Walvis Ridge –SW Atlantic), Mar. Micropaleontol., 69, 119–138, 2008.

Rickaby, R. E. M., Schrag, D. P., Zondervan, I., and Riebesell, U.: Growth rate dependence of Sr incorporation during calcification of *Emiliania huxleyi*, Global Biogeochem. Cy., 16(1), 1006, doi:10.1029/2001GB001408, 2002.

Richter, F. M. and Liang, Y.: The rate and consequences of Sr diagenesis in deep-sea carbonates, Earth Planet. Sc. Lett., 117(3–4), 553–565, 1993.

Ridgwell, R.: Interpreting transient carbonate compensation depth changes by marine sediment core modeling, Paleoceanography, 22, PA4102, doi:10.1029/2006PA001372, 2007.

Schneider, R. R., Muller, P. J., Ruhland, G., Meineke, G., Schmidt, H., and Wefer, G.: Late Quaternary surface temperature and productivity in the east-equatorial South Atlantic: response to changes in trade/ monsoon wind forcing and surface water advection, in: The South Atlantic: Present and Past circulation, edited by: Wefer, G., Berger, W. H., Siedler, G., and Webb, D. J., 527–551, Springer, Berlin, 1996.

CPD
7, 2089–2118, 2011

Productivity response of calcareous nannoplankton

M. Dedert et al.

Sexton, P. F., Norris, R. D., Wilson, P. A., Pälike, H., Westerhold, T., Röhl, U., Bolton, C. T., and Gibbs, S.: Eocene global warming events driven by ventilation of oceanic dissolved organic carbon, Nature, 471, 349-352, doi:10.1038/nature09826, 2011.
Stap, L., Sluijs, A., Thomas, E., and Lourens, L.: Patterns and magnitude of deep sea carbonate dissolution during the Eocene Thermal Maximum 2 and H2, Walvis Ridge, Southeastern Atlantic Ocean, Paleoceanography, 24, PA1211, doi:10.1029/2008PA001655, 2009.
Stap, L., Lourens, L., Thomas, E., Sluijs, A., Bohaty, S., and Zachos, J. C.: High-resolution deep-sea carbon and oxygen isotope records of Eocene Thermal Maximum 2 and H2, Geology, 38(7), 607–610, doi:101.1130/G30777.1, 2010.
Sloan, L. C. and Huber, M.: Eocene oceanic responses to orbital forcing on precessional time scales, Paleoceanography, 16(1), 101–111, 2000.
Stoll, H. M. and Bains, S.: Coccolith Sr/Ca records of productivity during the Paleocene-Eocene Thermal Maximum from the Weddell Sea, Paleoceanography, 18(2), 1049, doi:10.1029/2002PA000875, 2003.
Stoll, H .M. and Schrag, D. P.: Sr/Ca variations in Cretaceous carbonates: relation to productivity and sea level changes, Palaeogeogr. Palaeocl., 168, 311–336, 2001.
Stoll, H. M. and Shimizu, N.: Micro-picking of nannofossils in preparation for analysis by secondary ion mass spectrometry, Nat. Protoc., 4, 1038–1043, 2009.
Stoll, H. M. and Ziveri, P.: Separation of monospecific and restricted coccolith assemblages from sediments using differential settling velocity, Mar. Micropaleontol., 46(1–2), 209–221, 2002.
Stoll, H. M., Klaas, C., Probert, I., Ruiz-Encinar, J., and Garcia-Alonso, J. I.: Calcification rate and temperature effects on Sr partitioning in coccoliths of multiple species of coccolithophorids in culture, Global Planet. Change, 34, 153–171, 2002a.
Stoll, H. M., Rosenthal, Y., and Falkowski, P.: Climate proxies from the Sr/Ca of coccolith calcite: calibrations from continuous culture of *Emiliania huxleyi*, Geochim. Cosmochim. Acta, 66, 927–936, 2002b.
Stoll, H. M., Ziveri, P., Shimizu, N., Conte, M. H., and Theroux, S.: Relationship between coccolith Sr/Ca ratios and coccolithophore production and export in the Arabian Sea and Sargasso Sea, Deep-sea Res. II, 54, 581–600, doi:10.1016/j.dsr2.2007.01.003, 2007a.
Stoll, H. M., Shimizu, N., Archer, D., and Ziveri, P.: Coccolithophore productivity response to greenhouse event of the Paleocene-Eocene Thermal Maximum, Earth Planet. Sc. Lett., 258, 192–206, 2007b.

Stoll, H. M., Shimizu, N., Arevalos, A., Matell, N., Banasiak, A., and Zeren, S.: Insights on coccolith chemistry from a new ion probe method for analysis of individually picked coccoliths, Geochem. Geophy. Geosy., 8, Q06020, doi:10.1029/2006GC001546, 2007c.
Tremolada, F. and Bralower, T. J.: Nannofossil assemblage fluctuations during the Paleocene-Eocene Thermal Maximum at Sites 213 (Indian Ocean) and 401 (North Atlantic Ocean): palaeoceanographical implications, Mar. Micropaleontol., 52, 107–116, 2004.
West, S., Jansen, J. H. F., and Stuut, J.-B.: Surface water conditions in the Northern Benguela Region (SE Atlantic) during the last 460 kyr reconstructed from assemblages of planktonic forams, Mar. Micropaleontol., 51(3–4), 321–344, 2004.
Young, J. R. and Ziveri, P.: Calculation of coccolith volume and its use in carbonate flux estimates, Deep-Sea Res. II, Topical Studies in Oceanography, 47(9–11), 1679–1700, 2000.
Zachos, J. C., Lohmann, K. C., Walker, J. C. G., and Wise, S. W.: Abrupt climate change and transient climates during the Paleogene: A marine perspective, J. Geol., 101, 191–213, 1993.
Zachos, J. C., Kroon, D., and Blum, P.,: Proc. ODP Init. Rep., 208, available at: http://www-odp.tamu.edu/publications/208_IR/chap_01/chap_01.htm, 2004.
Zachos, J. C., Rohl, U., Schellenberg, S. A., Sluijs, A., Hodell, D. A., Kelly, D. C., Thomas, E., Nicolo, M., Raffi, I., Lourens, L., McCarren, H., and Kroon, D.: Rapid acidification of the ocean during the Paleocene- Eocene Thermal Maximum, Science, 308, 1611–1615, 2005.
Ziveri, P. and Thunell, R.: Coccolithophore export production in Guaymas Basin, Gulf of California: Response to climate forcing, Deep-Sea Res., 47(9–11), 2073–2100, 2000.
Ziveri, P., Thunell, R., and Rio, D.: Export production of coccolithophores in an upwelling region: results from San Pedro Basin, Southern California Bight, Mar. Micropaleontol., 24, 335–358, 1995.
Ziveri, P., De Bernardi, B., Baumann, K.-H., Stoll, H. M., and Mortyn, P. G.: Sinking of coccolith carbonate and potential contribution to organic carbon ballasting in the deep ocean, Deep-Sea Res. II, 54(5–7), 659–675, 2007.

CPD
7, 2089–2118, 2011

Productivity response of calcareous nannoplankton

M. Dedert et al.

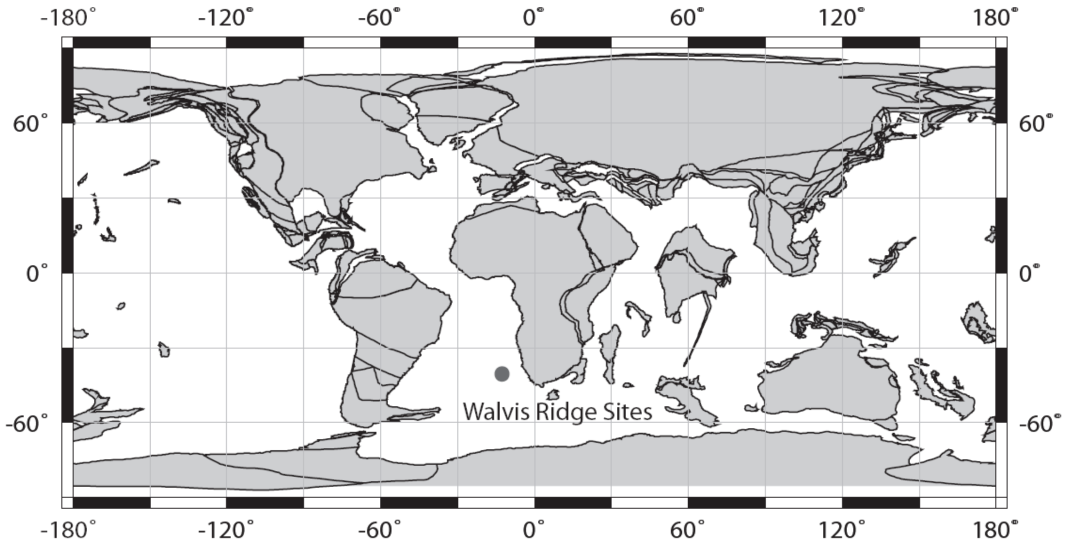

Fig. 1. Map showing the plate configuration of the Early Eocene with the location of ODP Site 1265 in the South Atlantic, Walvis Ridge.

CPD
7, 2089–2118, 2011

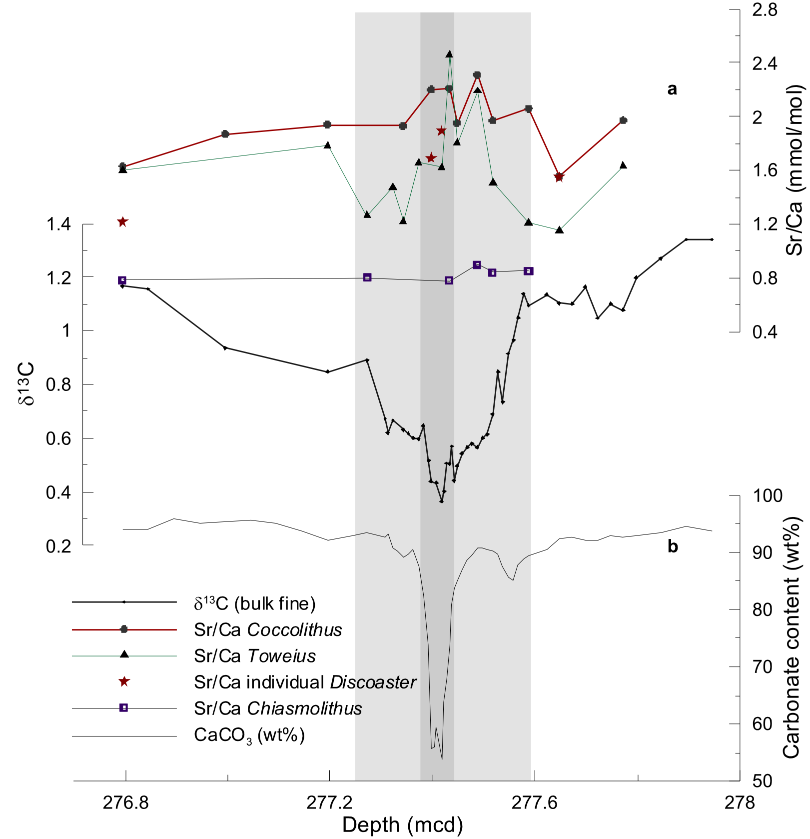

Fig. 2. (a) Sr/Ca productivity trend measured by ion probe in picked individuals or populations in correlation with the $\delta^{13}C$ (Dedert et al., 2011). *Coccolithus pelagicus* (grey dots), *Toweius* (black triangles), *Discoaster* (red stars), and *Chiasmolithus* (purple squares), **(b)** the carbonate content across the ETM2 interval. Light grey bar indicates the CIE, dark grey bar marks the dissolution horizon.

CPD
7, 2089–2118, 2011

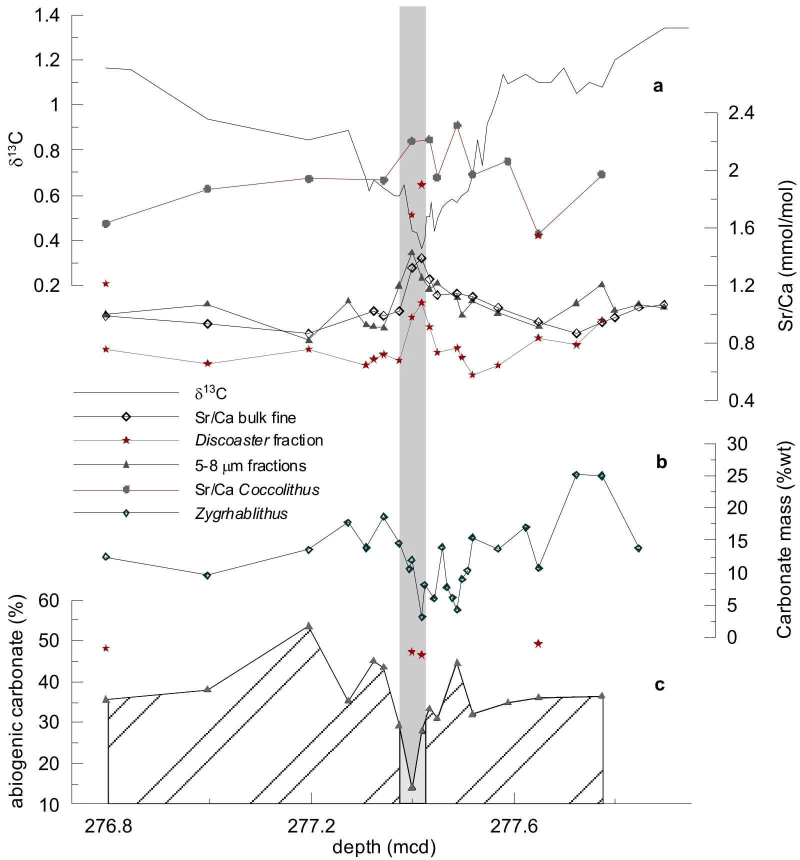

Fig. 3. **(a)** The Sr/Ca measured by ion probe in *Coccolithus* versus the Sr/Ca measured in the size fractions in correlation to the $\delta^{13}C$, **(b)** the mass contribution by *Zygrhablithus* to the 5–8 µm size fractions, and **(c)** the contribution of abiogenic calcite to the discoaster and 5–8 µm size fractions. Grey bar represents the *Elmo* horizon.

CPD
7, 2089–2118, 2011

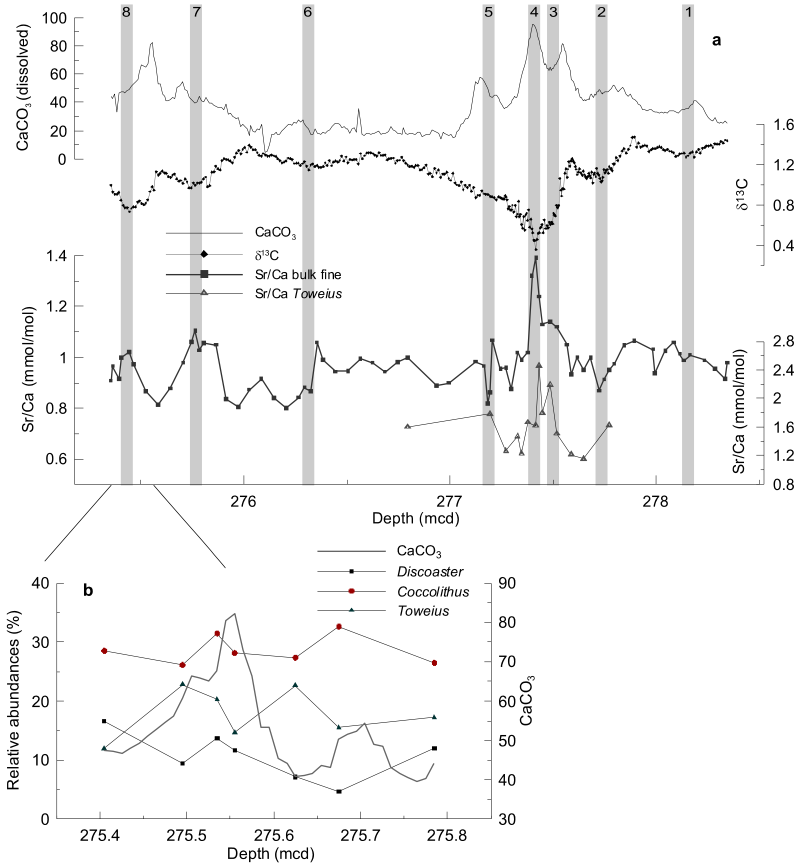

Fig. 4. **(a)** Long-term Sr/Ca productivity record measured in bulk fine sediments and Sr/Ca measured by ion probe in *Toweius*, in correlation to the calculated dissolved carbonate (Stap et al., 2009) and bulk δ^{13}C (Stap et al., 2009). Grey bars represent precessional cycles as identified by Stap et al. (2009), **(b)** the changes in assemblage composition across the H2 event.

CPD
7, 2089–2118, 2011

Productivity response of calcareous nannoplankton

M. Dedert et al.

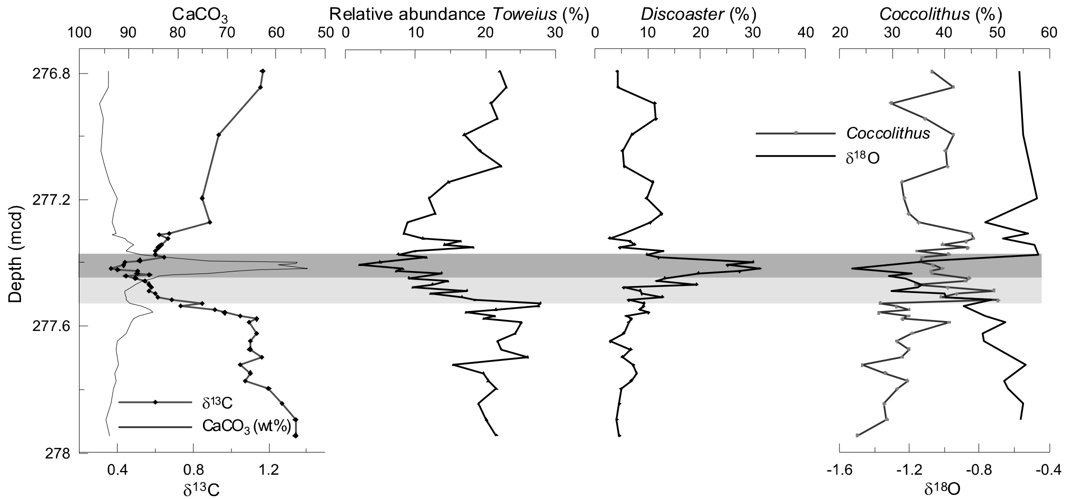

Fig. 5. The δ^{13}C (black rhomboids) and the carbonate content (grey line) plotted against the relative abundances of *Toweius*, *Discoaster* and *Coccolithus pelagicus* in correlation with the δ^{18}O measured in the 5–8 µm size fraction (Dedert et al., 2011). Dark grey bar indicates *Elmo* horizon, light grey bar indicates zone of salient increase in *Coccolithus* abundance.

CPD
7, 2089–2118, 2011

Productivity response of calcareous nannoplankton

M. Dedert et al.

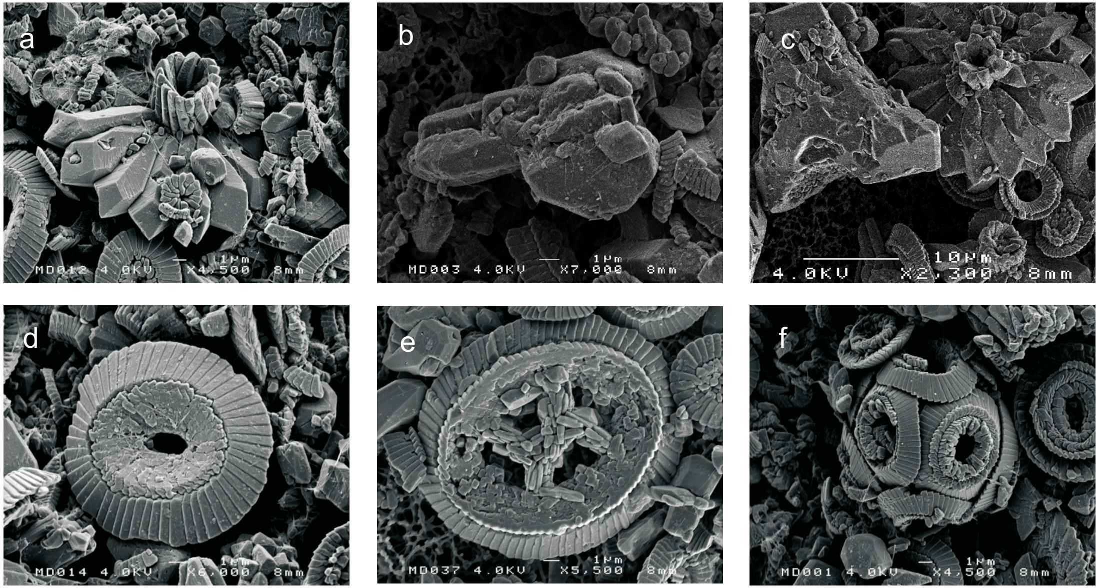

Plate 1. Preservation nannofossils ETM2 interval. **(a)** An overgrown *Discoaster*, **(b)** an overgrown *Zygrhablithus*, **(c)** an overgrown *Discoaster* and *Tribrachiatus*, **(d)** a placolith of *Coccolithus pelagicus*, **(e)** a placolith of *Chiasmolithus*, **(f)** a coccosphere of *Toweius*.

CPD
7, 2089–2118, 2011